

Design and Analysis of Circular Slotted Microstrip Patch Antenna

Kaustubh Bhattacharyya, Rupanda Thangjam, Sivaranjan Goswami, Kumaresh Sarmah and Sunandan Baruah

Abstract—This paper presents a novel complementary CPW-fed slotted microstrip patch antenna for operation at 2.4 GHz, 5.2 GHz and 6.3 GHz frequencies. The primary structure consists of the complementary split ring resonator slots on a patch and the design is fabricated on FR-4 epoxy substrate with substrate thickness of 1.6 mm. The described structure lacks the presence of a ground plane and makes use of a number of circular complementary SRRs along with rectangular slots on the radiating patch. The structure provides a wide bandwidth of around 390 MHz, 470 MHz and 600 MHz at the three bands with return losses of -11.5 dB, -24.3996dB and -24.4226 dB, respectively. The inclusion of the rectangular slots in the CSRR based slot antenna with staircase structure improved the performance with respect to return loss.

Keywords—microstrip, resonance frequency, complementary split ring resonators, impedance matching

I. INTRODUCTION

DESIGN of low profile, light weight antennas has remained a trend in the field of wireless communication for several decades. Microstrip antennas of various sizes and shapes have evolved. These antennas are basically used for short-range communication systems such as Bluetooth and Wi-Fi [1]. A microstrip antenna fed by a microstrip line provides advantages such as light and compact structure and easy fabrication process [2]. Although sizes of these antennas have been continuously reduced, low gain and bandwidth have been a challenge for microstrip antennas [3]. Conventional microstrip antennas have larger size and low bandwidth and are not appropriately applicable for WLAN applications that require miniaturized antennas [4]. Microstrip slot antennas are viewed as a plausible solution to this problem. These antennas are the complementary structures of microstrip antennas.

The radiation characteristics of a microstrip patch antenna are fundamentally affected by the presence of ground plane, slots in the ground plane and implementation of split ring resonators (SRR) and complementary split ring resonators (CSRR). SRRs are basically used when coupling between the antenna elements are required to be controlled and CSRRs

are implemented entirely for the enhancement of antenna parameters such as return loss, gain or bandwidth. It was seen that variation in the number of CSRRs in the ground plane as well presence of slots around the rings and staircase structures have significant influence on the operation of the antenna observed at different frequency bands. Complementary split ring resonators (CSRR) can be of two geometries: circular and square.

Antennas need to adapt to various WLAN environments. It is desirable that a WLAN antenna be able to operate at dual frequency bands [5], [6], popularly the bands covering (2.400-2.484) GHz (specified by IEEE 802.11b/g) and (5.150-5.350) GHz or (5.725-5.825) GHz (specified by IEEE 802.11a) [4]. A traditional approach to improve the performance of a microstrip antenna is by introducing one or more slots [7], [8] or by making use of split ring resonators or complementary split ring resonators to reduce both electrical size and return loss of the structure [9]. Li-Ming Si et al. describes a three SRR-based dual-band response antenna in [10].

In slot antennas, the two popular feeding techniques are microstrip lines and coplanar waveguides (CPW). For miniaturization process, CPW feeding is preferred over microstrip line feeding [11]. Bandwidth enhancement can be aided by implementation of CPW feeding [12], [13] as well as fractal structures [14], [15]. A bandwidth of up to 42 % achieved by CPW feeding at operating frequency of (2.26-3.29) GHz has been reported by Singh et al. in [16].

In this work, a complementary CPW structure is designed to feed a metamaterial inspired slot antenna. The radiating element is a modified complementary split ring resonator (CSRR) structure. A study of the effects of complementary-CPW feeding on the return loss and bandwidth has been presented. The design uses rectangular slots and a staircase structure on the ground plane for impedance matching.

II. EXPERIMENTAL DETAILS

The antenna is designed on a single-sided PCB of dimensions 32 mm x 28 mm x 1.6 mm. The substrate material is FR4 epoxy which has a relative permittivity (ϵ_r) of 4.4. The antenna consists of a modified CSRR structure as the radiating element etched from the copper ground plane on the FR4 epoxy substrate. The antenna is designed through four steps as follows.

A. Antenna with Split Ring Resonators

The antenna in this work has the radiating layer mounted on a substrate of planar dimensions 32 mm x 28 mm. A CPW

Kaustubh Bhattacharyya is with the Department of Electronics and Communication Engineering, School of Technology, Assam Don Bosco University, Assam, India. (e-mail: kaustubh.bhattacharyya@dbuniversity.ac.in)

Rupanda Thangjam is with the Department of Electronics and Communication Engineering, School of Technology, Assam Don Bosco University, Assam, India. (e-mail: thpanda11@gmail.com).

Sivaranjan Goswami and Kumaresh Sarmah are with the Department of Electronics and Communication Technology, Gauhati University, Assam, India. (e-mail: kumaresh4you8, sivgos@gmail.com).

Sunandan Baruah is with the Department of Electronics and Communication Engineering, School of Technology, Assam Don Bosco University, Assam, India (e-mail: sunandan.baruah@dbuniversity.ac.in).

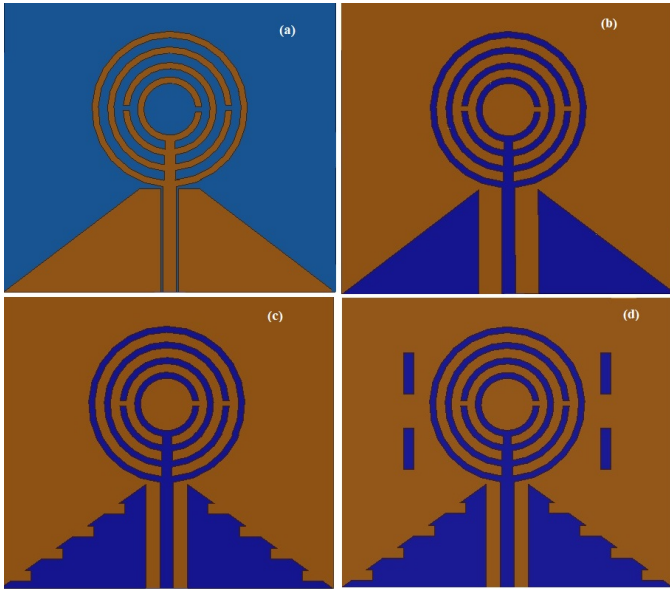


Fig. 1. Steps of design of the fabricated structure (a) CPW-fed structure with SRRs (b) Complementary-CPW-fed structure with CSRRs (c) Rectangular structures protruding out of the patch layer (d) Additional rectangular slots on the patch layer.

feed line is used to excite a structure of three concentric split rings encapsulated by a closed ring resonator as shown in Fig. 1(a). The rings have outer radii of 7.5 mm, 6 mm, 4.5 mm and 3.1 mm respectively. The thickness of each ring is 0.6 mm spaced by 0.9 mm. All the splits in the rings are of dimensions 0.5 mm x 0.6 mm. This antenna is designated as Antenna 1.

B. Antenna with Complementary Split Ring Resonators

In the next step, the entire structure of Antenna 1 was complemented so as to create a ground plane consisting of a CSRR inspired radiating element excited by a pair of microstrip feed lines. This antenna is designated as Antenna 2. The ground plane of the Antenna 1 is now becomes two triangular slots on the ground plane. The triangular slots on the ground plane along with the pair of parallel microstrip lines may be termed as a complementary CPW structure. Both of the triangular regions are of the same dimensions with the three sides 10 mm, 13.15 mm and 16.52 mm respectively. The structure is shown in Fig. 1(b).

C. Antenna with staircase structures on the end of the patch layer

Two staircase structures of rectangular geometry, one on each side of the CSRR structure, were added so that it protrudes out of the edges of the triangular part of the patch as shown in Fig. 1(c). Each of these structures has planar dimensions 2 mm x 1mm. This antenna is designated as Antenna 3.

D. Antenna with rectangular slots on the patch layer

Four rectangular slots were made on the ground plane, two on either of the CSRR as shown in Fig. 1(d). The slots have

a horizontal separation of 23 mm (lower edge to lower edge) and vertical separation of 7.3 mm (left edge to left edge). The rectangular slots aid in improving the impedance matching of the antenna thereby decreasing the return loss and helping in improved reception. This antenna is designated as Antenna 4.

E. Fabrication of the structure

The proposed design was simulated in ANSOFT HFSS 13.0 and results are tested. The presence of slots on the ground plane of a microstrip antenna affects antenna properties such as resonance frequencies, impedance matching and bandwidth [17]. Following the simulation results, the Antenna 4 is further considered for change in the structure design for any kind of improvement in its radiation parameters. The original structure i.e., Antenna 4 is simulated again with different horizontal and vertical distances between the rectangular slots. Further, the variation has been done in distance between pairs of slots, i.e. variation in horizontal distance has been done keeping the vertical distances constant between each pair of vertical slots. Similarly, variation in vertical distance (vd) has been done keeping the horizontal distances constant between each opposite pair of vertical slots. The distance between the rectangular slots was increased / decreased by a step of 2 mm till the stage it avoided intersection with the complementary split ring resonators or till it became too close to the edges of the substrate. Similarly, the distance between the rectangular slots was increased / decreased by a step of 2 mm keeping in consideration the slots did not intersect with the edges / parts of structure of the design. Following the simulation results, the design after the addition of the final feature (Antenna 4) was considered for fabrication. A 32 mm x 28 mm x 1.6 mm FR-4 epoxy material as the substrate. Four split ring resonators of same annular dimensions were then made on the patch layer. A feed line connecting all the split ring resonators was designed. Slots were made on the patch layer, four on each side of the feed line. An extra copper layer of same thickness as that of the split ring resonators was then laid out on top of the substrate. The first layers are etched out from the copper layer to form complementary structures and the extra four slots of dimensions given in the Table I are etched from the patch layer. The feed point is given in the XZ-plane to make contact with the two feed line structures. The following Table I sums up the dimensions of the proposed model.

The top view of the fabricated antenna is shown in Fig. 2

Further the performance of the Antenna4 is studied in the absence of the staircase structures in the ground plane and designated as Antenna 5. The top-view of the structure is shown in Fig. 3. The top-view of the fabricated model (Antenna 5) is shown in Fig. 4.

III. RESULTS AND DISCUSSION

The step-by step simulation results with respect to return losses are shown in Fig. 5. Fig. 5(a) shows that the Antenna 1 resonates at 3.6 GHz with a wide bandwidth of 1.12 GHz but with a very high return loss of -13.1969 dB. Antenna 2 is a tri-band antenna which resonates at 2.6 GHz, 5.1 GHz and 6.1 GHz with corresponding return losses of -24.1221

TABLE I
DIMENSIONS OF THE ANTENNA

Dimension within the structure	Value
Length of the patch	32 mm
Width of the patch	28 mm
Thickness of the patch	0.035 mm
Thickness of substrate layer	1.6 mm
Dielectric constant of substrate	4.4
Outer radius of the outermost CSRR	7.5 mm
Inner radius of the outermost CSRR	6.9 mm
Outer radius of the second CSRR	6 mm
Inner radius of the second CSRR	5.4 mm
Outer radius of the third CSRR	4.5 mm
Inner radius of the third CSRR	3.9 mm
Outer radius of the innermost CSRR	3.1 mm
Inner radius of the innermost CSRR	2.5 mm
Width of each annuli	0.6 mm
Gap between consecutive annuli	0.9 mm
Length of each rectangular slot	4 mm
Width of each rectangular slot	1 mm
Length of each protruding structure	2 mm
Width of each protruding structure	1 mm

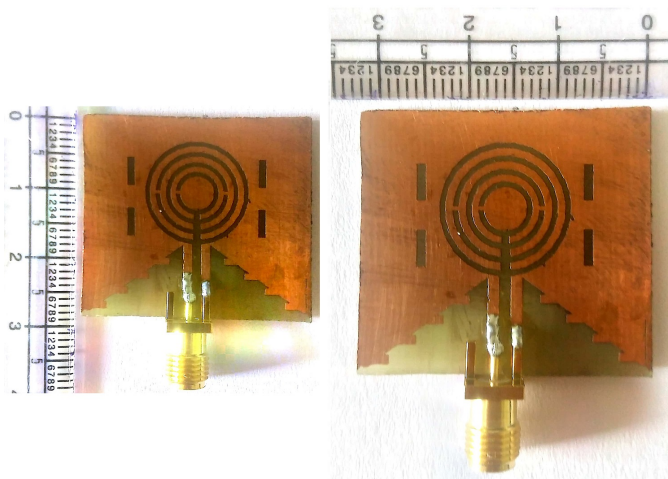


Fig. 2. Top-view of the fabricated structure of the proposed antenna



Fig. 3. Top-view of the Antenna 4 without staircase structures (Antenna 5)

dB, -16.1035 dB and -20.8792 dB, respectively. However, the bandwidth gets reduced to 287 MHz, 285 MHz and 318 MHz at the three resonance frequencies (Fig. 5(b)). The presence

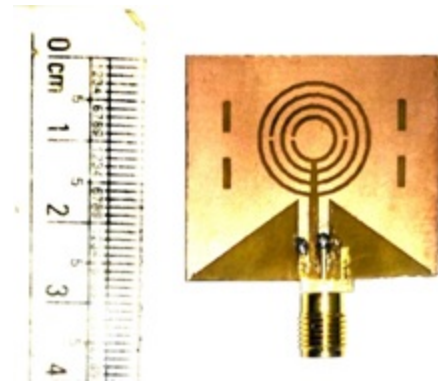


Fig. 4. Top-view of the fabricated Antenna 5

of the staircase structures in Antenna 3 resulted in the shift of resonance frequencies from 2.6 GHz and 5.1 GHz to 2.5 GHz and 5 GHz respectively along with a 6.1 GHz resonance frequency as in Antenna 2. The return losses at the resonance frequencies are -29.4854 dB, -23.7135 dB and -20.8279 dB, with corresponding bandwidths 292 MHz, 321 MHz and 291 MHz, respectively (Fig. 5(c)). It is observed that, although there is a corresponding shift in frequency of around 0.1GHz results in Antenna 3 compared to Antenna 2, but there is a corresponding decrease in return loss of about 5dB and 7dB in first two frequencies respectively. Also there is an increase in bandwidth of 5MHz and 36MHz respectively in first two cases. The return losses of Antenna 4 were significantly reduced to -35.9897 dB, -43.8995 dB and -22.4346 dB at the three resonance frequencies 2.5 GHz, 5.1 GHz and 6.1 GHz, along with bandwidths of 280 MHz, 310 MHz and 280 MHz, respectively (Fig. 5(d)). It is observed that, with the incorporation of the vertical slots in Antenna 4 results decrease in return loss of around 6dB, 20dB, and 2dB respectively compared to Antenna 3 without affecting the bandwidth much.

Figure 6 shows the gain of the final structure i.e. of Antenna 4. The gain is observed to be maximum in the Z-direction.

In order to estimate the reliability of the simulation results, the fabricated structure was analyzed using a Vector Network Analyzer (Rohde & Schwarz made ZNB20) connected through a 50 Ω SMA connector. The performance of the fabricated Antenna as recorded by the VNA has been shown in the form of return loss and Smith chart in Fig. 7. As observed from VNA-testing, Antenna 4 resonates at 2.56 GHz, 5.19 GHz and 6.28 GHz with reported return losses of -22.2051 dB, -24.5796 dB and -21.8712 dB respectively. Also, the Smith chart shows that Antenna 4 matches the medium with impedances of 53.247 , 43.630 and 57.768 at the three resonance frequencies, respectively. Following the values, the antenna matches the medium best at 2.56 GHz frequency. Fig. 8 shows the return loss of the fabricated Antenna 4 along with the simulated result.

A comparison of the performance of the simulated and fabricated model of Antenna 4 is given Table II. It is seen that, although the return loss is minimum at the resonating frequency 5.1GHz in both simulation and measurement, but also the return loss at other two frequencies are less than -

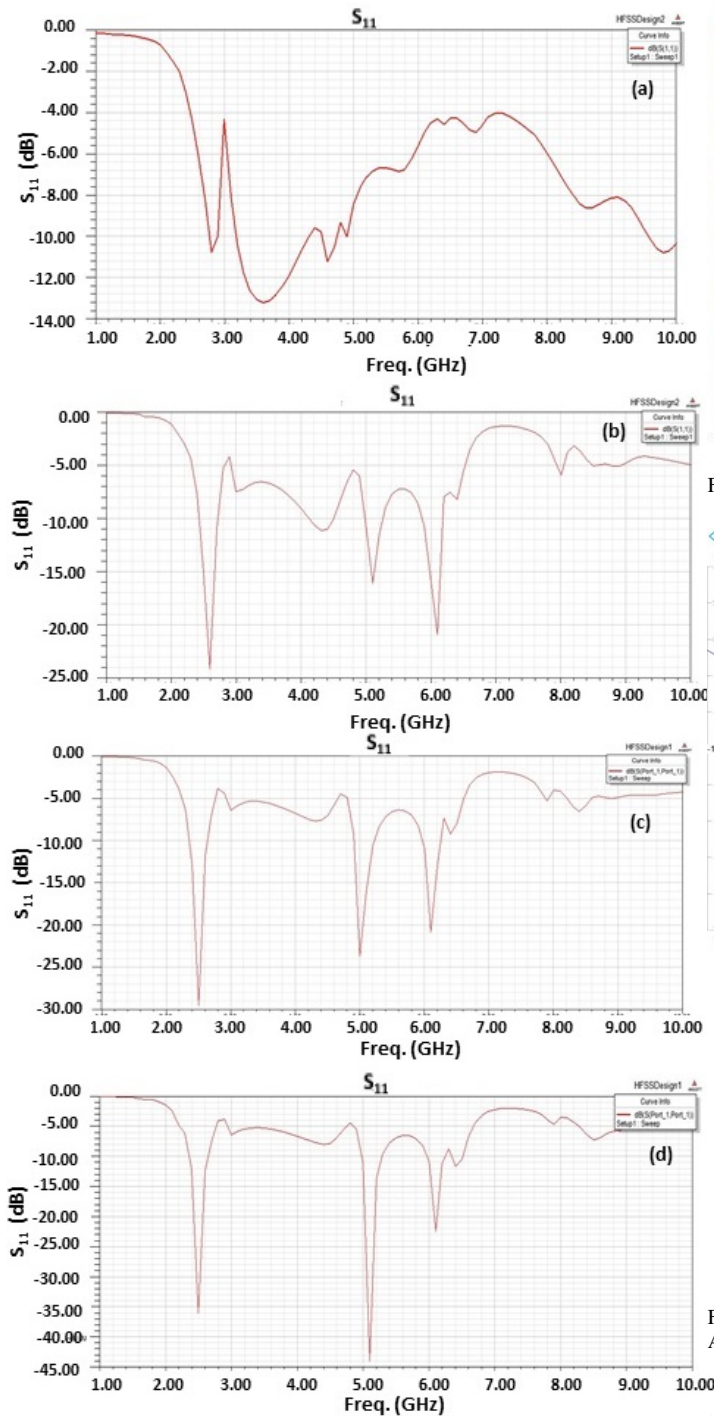


Fig. 5. (a) Return Loss from structure of Antenna 1, (b) Return Loss from structure of Antenna 2, (c) Return Loss from structure of Antenna 3 and (d) Return Loss from structure of Antenna 4.

10dB. There is a slight difference in values of different parameters between simulation and measurement. It may be because of the imperfection of the fabrication of the structure, which can be further tuned towards perfection. Thus the bandwidths observed at the three bands from simulation are 280 MHz, 310 MHz and 280 MHz as opposed to the measured 390 MHz, 470 MHz and 600 MHz, respectively. Thus, Antenna 4 could

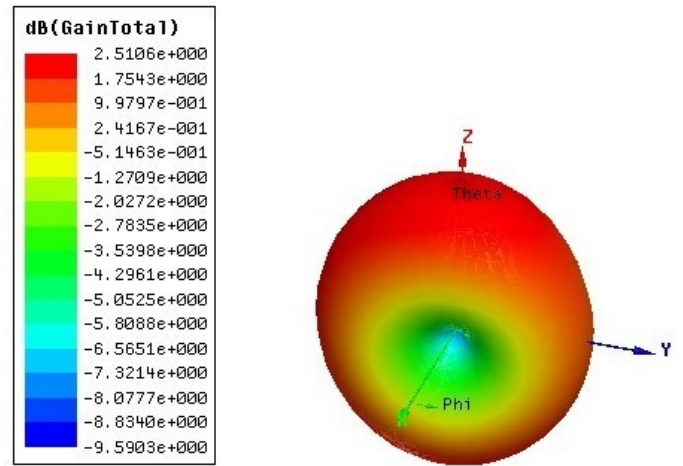


Fig. 6. Gain from structure of Antenna 4

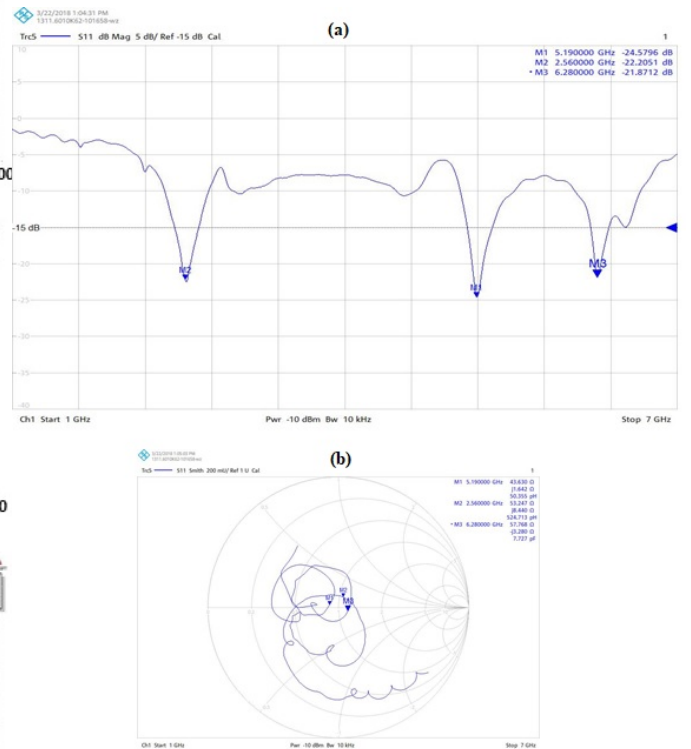


Fig. 7. (a) Return loss (b) Smith chart shown by the VNA from testing of Antenna 4

be expected to give high bandwidth in operation at the three bands.

Table III shows the impedances (Z_0) of Antenna 4 when it is observed to be operating at different resonance frequencies.

Although the values of impedance are not 50Ω (as should be in the ideal case), the values at each resonance frequencies are very close to 50Ω . Thus, with respect to both return loss and impedance matching, the simulation and measurement results of Antenna 4 are in fair agreement with each other.

The radiation patterns observed from simulation as well as from measurement of Antenna 4 are shown in Fig. 9.

The two radiation patterns have been presented with focus on the azimuthal and the elevation plane only i.e. at $\varphi = 0^\circ$

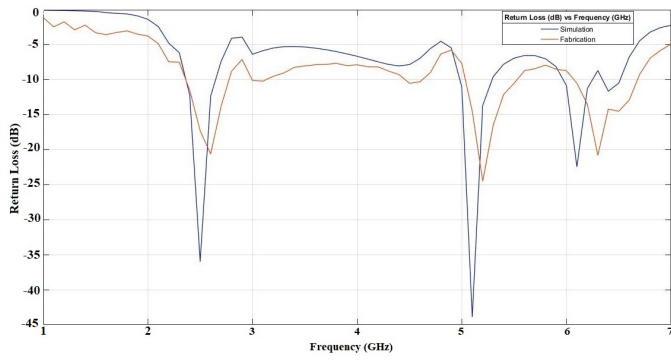


Fig. 8. Comparison of return loss of simulated and fabricated model

TABLE II
COMPARISON OF SIMULATION AND MEASUREMENT VALUES OF PARAMETERS OF ANTENNA 4

Solution frequency (2.4 GHz) and f_r (GHz)		S_{11} (dB)		Bandwidth (MHz)	
Simulated	Measured	Simulated	Measured	Simulated	Measured
2.4	2.4	-12.2006	-11.5	280	390
2.5	2.56	-35.9897	-22.2051		
5.1	5.19	-43.8995	-24.5796	310	470
6.1	6.28	-22.4346	-21.8712	280	600

TABLE III
IMPEDANCE OF ANTENNA 4 AS OBSERVED AT DIFFERENT RESONANCE FREQUENCIES

f_r (GHz)	Z_0 (Ω)
2.56	53.247
5.19	43.630
6.28	57.768

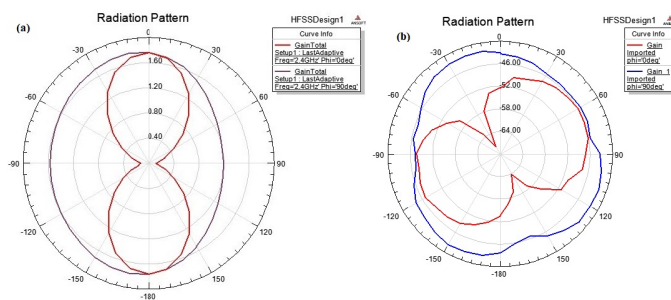


Fig. 9. (a) Radiation pattern of the Antenna 4 observed from simulation, (b) Radiation pattern of the Antenna 4 obtained from measurement.

and $\varphi = 90^\circ$. The measured pattern along the elevation plane (i.e. the red curve in Figure 8(b)) is observed to be off from the respective axis at an angle. This is expected to be caused by the capacitance caused by the asymmetry of the design as in there is absence of metal layer on the back side of the substrate, thus allowing the radiation from the ground plane

to penetrate the substrate and getting distributed into irregular directions.

The simulated result of return loss of Antenna 5 is shown Fig. 10. The performance of Antenna 5 as recorded by the VNA has been shown in the form of return loss and Smith chart is shown in Fig. 11.

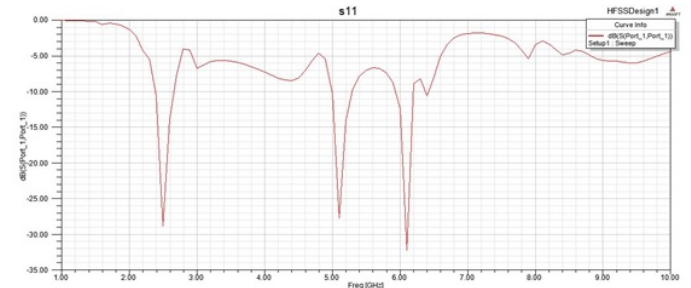


Fig. 10. Return loss observed from the simulation of Antenna 5

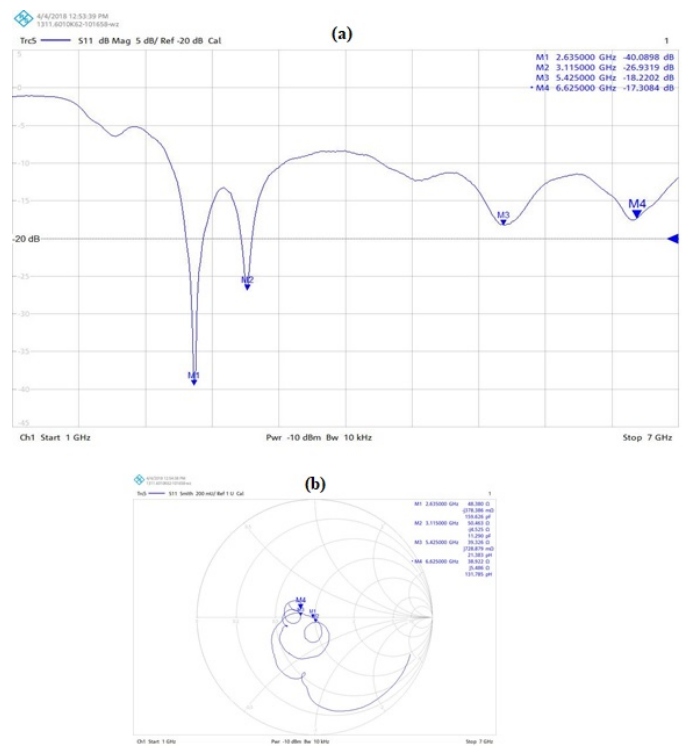


Fig. 11. (a) Return loss (b) Smith chart shown by the VNA from testing of Antenna 5

As observed from VNA-testing, Antenna 5 resonates at 2.63 GHz, 5.42 GHz and 6.62 GHz with reported return losses of -22.2051 dB, -24.5796 dB and -21.8712 dB respectively. Also, the Smith chart shows that Antenna 5 matches the medium with impedances of 48.380 Ω , 39.326 Ω and 38.992 Ω at the three resonance frequencies, respectively. Following the values, the antenna matches the medium best at 2.63 GHz frequency. Fig. 12 gives a comparison of the resonance frequencies observed from the simulation and testing of the fabricated Antenna 5.

Table IV shows a comparison of the resonance frequencies and values of the parameters return and bandwidth of the

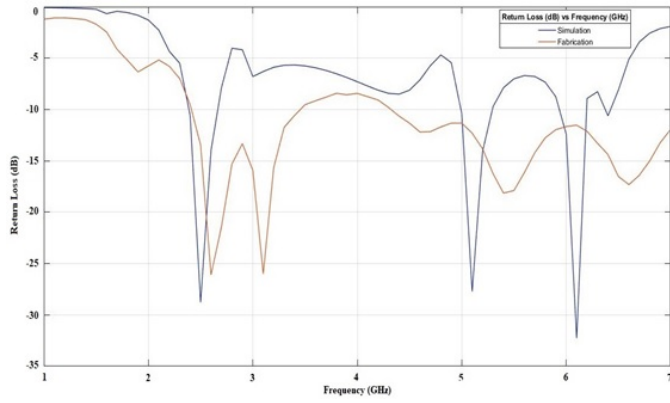


Fig. 12. Comparison of return losses observed from simulation and VNA-testing of Antenna 5

Antenna 5. The bandwidths observed at the three bands from

TABLE IV
COMPARISON OF SIMULATION AND MEASUREMENT VALUES OF PARAMETERS OF ANTENNA 5

Solution frequency (2.4 GHz) and f_r (GHz)		S_{11} (dB)		Bandwidth (MHz)	
Simul-ated	Measu-red	Simulated	Measured	Simul-ated	Measu-red
2.4	2.4	-10.5976	-9.5333	276	1020
2.5	2.63	-38.7688	-40.0898		
5.1	5.42	-27.7091	-18.2202	301	3070
6.1	6.62	-32.2538	-17.3084	261	

simulation are 276 MHz, 301 MHz and 361 MHz as opposed to the measured to 1020 MHz and 3070 MHz observed from fabrication, respectively. Thus, Antenna 2 could be expected to give high bandwidth in operation at the three bands.

Further, Fig. 13 presents the radiation patterns obtained from the simulation and that observed from the measurement of Antenna 5.

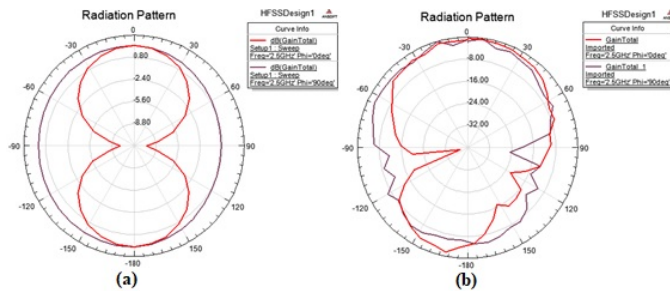


Fig. 13. (a) Radiation pattern of Antenna 3 observed from simulation (b) Radiation pattern of Antenna 5 obtained from measurement

The two radiation patterns have been presented with focus on the azimuthal and the elevation plane only i.e. at $\varphi = 0^0$ and $\varphi = 90^0$. The measured pattern along the elevation plane (i.e. the red curve in Fig. 13 (b)) is observed to be off from the respective axis at an angle. This is expected to be caused

by the capacitance caused by the asymmetry of the design as in there is absence of metal layer on the back side of the substrate, thus allowing the radiation from the ground plane to penetrate the substrate and getting distributed into irregular directions. Overall, it is clear that aside from the small shifts in the different resonance frequencies and impedance matching values, the return losses provided by the structure are in agreement with each other. However, the bandwidths provided by the fabricated structure have increased from the MHz scale to the GHz scale, which is an advantage for operation in both the lower and upper ranges of the wireless spectrum.

Table V shows the overall comparison of the measurement values of the two antennas (Antenna 4 and Antenna 5) as noted from the VNA testing.

TABLE V
COMPARISON OF SIMULATION AND MEASUREMENT VALUES OF PARAMETERS OF ANTENNA 5

Solution frequency (2.4 GHz) and f_r (GHz)		S_{11} (dB)		Bandwidth (MHz)	
Antenna4	Antenna5	Antenna4	Antenna5	Antenna4	Antenna5
2.4	2.4	-11.5	-9.5333	390	1020
2.56	2.63	-22.2051	-40.0898		
5.19	5.42	-24.5796	-18.2202	470	3070
6.28	6.62	-24.4226	-17.3084	600	

From the above Table V, it is clear that although high bandwidth is an advantage achieved from the third structure, it basically does not resonate within the standard WLAN frequency ranges. Therefore, overall analysis indicates that the staircase structure in the ground plane aids in the addition of impedance matching leading to better antenna performance.

IV. CONCLUSION

Slots are also introduced on the patch layer of a microstrip antenna in order to enhance its performance in terms of return loss and bandwidth. Different circular CSRR based antennas are presented in this paper, and finally two of which were fabricated with one make use of staircase structures in the ground plane. The first fabricated one resonates at 2.56 GHz, 5.19 GHz and 6.28 GHz with corresponding return loss of -22.2051 dB, -24.5796 dB and -21.8712 dB respectively. Thesecond fabricated structure, with vertical slots, had its resonance condition at 2.63 GHz, 5.42 GHz and 6.62 GHz with corresponding return loss -40.0898dB, -18.2202 dB and -17.3084 dB respectively. The second fabricated structure, in the absence of staircase structures, had its resonance condition shifted slightly towards the higher frequencies. Also, bandwidths recorded to be provided by the two antennas were fairly much higher than observed in the simulation process. comparing both it is concluded that the staircase structure in the ground plane aids in the addition of impedance matching leading to better antenna performance. The incorporation of vertical slots in a CSRR based slot antenna can improve the performance in terms of return loss. The CSRR based tri-band

antenna with vertical slots presented here provides maximum bandwidth of 310 MHz at a resonating frequency of 5.1 GHz from simulation and 600 MHz at a resonating frequency of 6.28 GHz from fabricated structure.

ACKNOWLEDGMENT

Authors would like to acknowledge Assam Don Bosco University, Assam, India and Gauhati University, Assam, India for providing the necessary resources for compiling this paper.

REFERENCES

- [1] Lal Chand Godara, "Handbook of Antennas in Wireless Communication", *The Electrical Engineering and Applied Signal Processing Series*, (2001).
- [2] Balanis C. A., "Handbook of Antennas in Wireless Communication", *John Wiley & Sons, Inc.*, (1997).
- [3] A. Kundu, Bappaditya Roy, S. Batabyal, U. Chakraborty, A. K. Bhat-tacharjee, "A Coaxial fed Compact Rectangular Microstrip Antenna with Multi-layer Configuration for WLAN2.4/5.2/5.8 GHZ band Applications", *International Conference on Industrial and Information Systems (ICIIS)*, (2014).
- [4] S. Gai, Y. C. Jiao, Y. B. Yang, C. Y. Li, and J.-G. Gong, "Design of A Novel Microstrip-Fed Dual-Band Slot Antenna for WLAN applications", *Progress In Electromagnetics Research Letters*, 13, 7581, (2010).
- [5] Shams, K. M. Z., M. Ali, and H. S. Hwang, "A planar inductively coupled bow-tie slot antenna for WLAN application", *Journal of Electromagnetic Waves and Applications*, 20 (7), 861-871, (2006).
- [6] Eldek, A. A., A. Z. Elsherbeni, and C. E. Smith, "Square slot antenna for dual wideband wireless communication systems", *Journal of Electromagnetic Waves and Applications*, 19 (12), 1571-1581, (2005).
- [7] G. BiffiGentili, P. Piazzesi, and C. Salvador, "Dual-band slot-loaded patch antenna", *In Microwaves, Antennas and Propagation, IEEE Proceedings*, 142 (3), 225-232. IET, (1995).
- [8] G. F. Khodaei, J. Nourinia, and C. Ghobadi, "A practical miniaturized u-slot patch antenna with enhanced bandwidth", *Progress In Electromagnetics Research B*, 3, 47-62, (2008).
- [9] Sivararjan Goswami, Kumaresh Sarmah, Angana Sarma, Kandarpa Kumar Sarma, Sunandan Baruah, "Slot Loaded Square Patch Antenna with CSRR at Ground Plane", *Microelectronics, Computing and Communications (MicroCom)*, (2016).
- [10] Li-Ming Si, Weiren Zhu, Hou-Jun Sun, "A Compact, Planar, and CPW-Fed Metamaterial-Inspired Dual-Band Antenna", *IEEE Antennas and Wireless Propagation Letters*, 12, (2013).
- [11] Abeesh, T. and M Jayakumar, "Design and studies on dielectric resonator on-chip antennas for millimeter wave wireless application", *Proceeding of 2011 International Conference on Signal Processing Communication Computing and Networking Technologies (ICSCCN 2011)*, IEEE, (2011).
- [12] Chen, X., Han, L., Chen, X., Zeng, Q., and Zhang, W., "A Wideband Coplanar Waveguide Antenna Array with Series Feed", *IEEE Antennas and Wireless Propagation Letters*, 16, 565-568, (2017).
- [13] Abdullah, B., Suryani, S., and Bannu., "Microstrip antenna slot double-bowtie five-array model with coplanar waveguides for 5.8 GHz communication", *In AIP Conference Proceedings*, 1801 (1), 050004. AIP Publishing. (2017).
- [14] Nugraha, I. P. E. D., Surjati, I., and Alam, S., "Miniaturized Minkowski-Island Fractal Microstrip Antenna Fed by Proximity Coupling for Wireless Fidelity Application", *TELKOMNIKA (Telecommunication Computing Electronics and Control)*, 15 (3), (2017).
- [15] Sedghi, M. S., Naser-Moghadasi, M., and Zarrabi, F. B., "Microstrip antenna miniaturization with fractal EBG and SRR loads for linear and circular polarizations", *International Journal of Microwave and Wireless Technologies*, 9 (4), 891-901, (2017).
- [16] Sedghi, M. S., Naser-Moghadasi, M., and Zarrabi, F. B., "Broadband CPW Fed Slotted Ground Antenna", *IOSR Journal of Electronics and Communication Engineering (IOSRJECE)*, (2), 36-39, (2012).
- [17] Shivnarayan, Shashank Sharma, Babau R Vishwakarma, "Analysis of slot-loaded rectangular microstrip patch antenna", *Indian Journal of Radio and Space Physics*, 34 (2), 424-430, (2005).